EXPERIMENTS ON FREEZE-BONDING BETWEEN ICE BLOCKS IN FLOATING ICE RUBBLE

by

J. A. Schaefer and R. Ettema

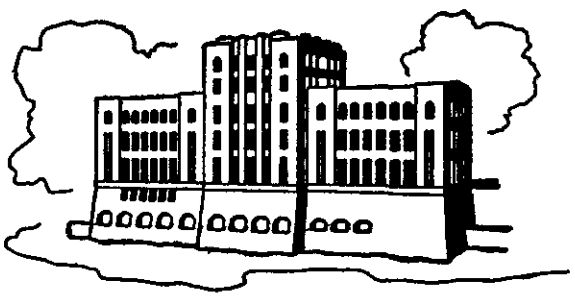

IIHR Report No. 296

Iowa Institute of Hydraulic Research
The University of Iowa
Iowa City, Iowa 52242 USA

December 1985

EXPERIMENTS ON FREEZE-BONDING BETWEEN ICE BLOCKS IN FLOATING ICE RUBBLE

by

J. A. Schaefer and R. Ettema

IIHR Report No. 296

Iowa Institute of Hydraulic Research
The University of Iowa
Iowa City, Iowa 52242 USA

December 1985

ABSTRACT

Series of experiments were conducted with the aim of determining the influences of the following factors on freeze-bonding between contacting ice blocks in floating ice rubble: pressure normal to the contact plane, period and area of contact, and salinity of the water in which freeze-bonding occurred. Freeze-bonding between ice blocks in air was also investigated.

The experiments were conducted with water and air temperatures of about 0° and normal pressures, between ice blocks, up to 4 kPa. This range of normal pressures may occur hydrostatically between ice blocks in layers of floating ice rubble up to about 10-m thick, or in 2 to 3-m-thick layers which are in a passive Rankine state of pressure.

The experiments show that stronger freeze-bonds develop between ice blocks in distilled water, tap water and water from the Iowa River than develop between ice blocks contacting in air at 0°C. However, stronger freeze-bonds develop in air at 0°C than develop between ice blocks in 0°C saline (NaCl) solutions with salinities in excess of 12.5% by weight. The strength of freeze-bonding increases linearly with contact period for ice blocks in distilled, tap and river waters, but do not increase with contact period for ice blocks contacting in saline solutions or in air.

The results of the experiments may contribute to explanations of the shear strength behavior of a layer of floating ice rubble. For example, thicker layers of ice rubble may show greater cohesive behavior, because normal pressures and thus freeze-bond strengths increase with layer thickness.

ACKNOWLEDGEMENTS

This study was funded jointly by The University of Iowa and the National Science Foundation under Grant No. CEE81-09252.

Dr. J. Schaefer conducted this study while on summer leave from his position as Professor of Physics and Engineering Science at Loras College, Dubuque, Iowa.

TABLE OF CONTENTS

LIST OF FIGURES

LIST OF TABLES

EXPERIMENTS ON FREEZE-BONDING BETWEEN ICE BLOCKS IN FLOATING ICE RUBBLE

I. INTRODUCTION

Laboratory studies (e.g., by Uzuner 1974 and Tatinclaux and Cheng 1978) show that the shear strength and deformation behavior of a relatively thick (block size is small compared to layer thickness) layer of floating ice rubble may be described using a Mohr-Coulomb relationship involving a term for apparent cohesion. Additionally, these studies show that shear rate strongly affects the shear strength of a layer of ice rubble. One explanation for the cohesive behavior of a layer of floating ice rubble, and for the effect of shear rate on shear strength, is the development of freeze-bonds between adjoining, contacting ice blocks.

A. Scope of Study. Consider two ice blocks, both with side dimensions of unity, brought in contact as illustrated in figure 1. If the blocks are loaded with a normal force which produces a normal pressure σ, then subsequent to a period t after application of σ, the two blocks would have to be separated at their interface by a shearing force which produces a shear stress τ across the bond. In order for the blocks to be separated, τ would have to overcome the shear strength of a freeze-bond between the blocks.

The aim of this study is to determine the dependence of freeze-bond strength τ on normal pressure σ, contact time t, fluid — air, pure water, or saline water — surrounding the two ice blocks, and contact area. The range of normal pressures was limited to a maximum value of 4kPa, which is within the range of pressures that may develop in layers of ice rubble up to about 9-m thick and in a neutral Rankine state. The fluid--air, water--surrounding the blocks was held at 0°C.

B. Background. It is helpful to the understanding of the ensuing study if the nature of ice-rubble strength is briefly outlined. Immediately after its formation, a layer of floating ice rubble undergoing deformation behaves

similarly to a deformed granular medium. Its shear strength results from the mechanical friction and rolling resistance and cohesion between ice blocks in contact. For this reason, most attempts (e.g., Prodanovic 1979, Hellman 1984) to date at formulating shear strength of rubble have expressed it in the form of the Mohr-Coulomb relationship;

$$\tau = c + \sigma \tan \phi \ , \qquad (1)$$

in which τ = shear strength; c = cohesive intercept; σ = compressive stress normal to the shear plane; and, φ = angle of internal resistance.

As soon as the rubble comes to rest after its formation, adjacent ice blocks may start to freeze to each other at their points of contact, and form a rigid matrix known as consolidated rubble. Because most of the rubble is submerged, the surfaces of the ice blocks are at the melting temperature. Consequently, freezing can occur with little or no heat transfer. This freezing diffusion of submerged boundaries into each other begins immediately and continues so that, with the passage of time, the freeze-bonds strengthen and the shear strength of the consolidated rubble increases.

It is evident that any factor which leads to more intimate contact between ice blocks will produce more extensive surface-contact area between ice blocks and increase the shear strength of the layer, as well as, possibly, the freeze-bond between the ice blocks. Therefore, τ will be a function of σ, not only for its role of increasing the mechanical friction of the rubble, but also because a large σ will decrease rubble porosity, p, and increase surface contact area and, thereby, also c. The intrinsic cohesion, c, of a layer of floating ice rubble is a function of contact period, t, compressive pressure σ, as well as shape, roughness and packing of ice blocks. Additionally, c will be influenced by the temperature and salinity of the water in which the layer of ice rubble floats.

Understanding the nature of freeze-bonding between ice blocks is important for understanding the shear-strength and deformation behavior of a floating layer of ice rubble. Surprisingly little is known about the intrinsic cohesion between blocks of ice, and there have apparently been no investigations on the strength of bond formed between ice block on ice

block. A considerable number of studies (e.g., by Oksanen 1983) have been conducted to determine the strength of ice bonding to other materials.

Merino (1974), Uzuner and Kennedy (1976), Mellor (1980) and others have shown that the vertical component of the internal stresses with a layer of floating ice rubble can be written as

$$\sigma_z = (1-p)\rho_i g z \quad , \qquad \text{for} \quad 0 \leq z \leq (1 - \rho_i/\rho_w)h \ , \tag{2a}$$

and

$$\sigma_z = (1-p)(\rho_w - \rho_i)\, g\, (h-z) \quad , \text{ for } (1 - \rho_i/\rho_w)h \leq z \leq h \ , \tag{2b}$$

in which p = porosity of the layer; ρ_i and ρ_w = the densities of the layer of ice blocks and of water, respectively; h = total thickness of layer of ice rubble; and z = distance below surface of ice rubble layer. Figure 2 depicts a simplifed layer of ice rubble and shows the terms in (2a) and (2b). If the following values are assumed, p = 0.40, $\rho_w = 10^3$ kg/m^3, $\rho_i = 0.92 \times 10^3$ kg/m^3, then (2a) becomes

$$\sigma_z = 5.42z \qquad \ldots \text{ (kPa, with z in m)}, \tag{3a}$$

and (2b) becomes

$$\sigma_z = 0.471\ (h-z) \qquad \ldots \text{ (kPa, with h and z in m)}, \tag{3b}$$

The relationship between σ_z and z is indicated in figure 2. For the present study, the development of freeze-bonds is examined for compressive, or normal, pressures up to about 4 kPa. As is suggested in figure 2, this range of compressive pressures is commensurate with vertical stress, σ_z, acting through ice-rubble layers up to 10-m thick. With regard to lateral pressures acting through a layer of ice rubble, 0 to 4 kPa is commensurate with passive pressures acting through layers up to (10 m)/K_p thick. The coefficient of Rankine-state passive pressure, K_p, varies from about 3 to 8 for values of angle of internal resistance ranging from 30° to about 50° (Mellor, 1980).

The range of normal pressures used for the present study covers much of the range for layers of floating ice rubble commonly encountered in nature.

II. FREEZE-BONDING BETWEEN ICE BLOCKS

The phenomenon of freeze-bonding between ice blocks, or ice particles, is well known and has been investigated by such noted physicists as Michael Faraday and James Thomson. Most of research effort has been concentrated on investigations of freeze-bonding between suspended particles of ice (e.g., Faraday 1859, Thomson 1861), especially spheres of ice (e.g., studies by Nakaya and Matsumoto 1954, Jensen 1956, Kingery 1960, Kuroiwa 1961, Hobbs and Mason 1964).

The mechanism causing ice pieces to be adhesive, and hence the cohesive behavior of a layer of ice rubble, has been the topic of considerable interest and debate. Hobbs (1974) and Pounder (1965), among others, provide detailed discussions on freeze-bonding. Faraday ascribed freeze-bonding to the freezing of a "liquid-like" layer (term used by Hobbs) at the interface of two moist ice pieces. Thomson attributed freeze-bonding to pressure melting at the contact between two ice pieces.

More recently, the process of sintering, or cold welding, has been used to explain the growth of a freeze-bond between contacting ice pieces, especially for pieces surrounded by air. Kingery (1960) and Kuroiwa (1961), for example, use this explanation for freeze-bonding.

When two contacting ice pieces are pressed against each other (e.g., as in figure 1), pressure melting may also come into play. If the pressure remains on the ice pieces, pressure melting may cause the two ice pieces to seat in closer contact, and the pressure may cause a sandwiched film of water of be squeezed from between the ice pieces. The upshot of the pressure would be the more rapid development of a stronger freeze-bond.

If the two moist ice pieces are surrounded by air, freezing of the water film at the contact may cause the two pieces to become fused to one another. Thereafter, the fusion would grow principally through the action of diffusion through the vapor phase of water, as is proposed by Hobbs and Mason (1964).

If a freeze-bond did not form between two ice blocks, static friction would have to be overcome in order to slide them apart. The shear stress to overcome static friction and separate the two blocks can be stated as

$$\tau_f = \mu_s \sigma \ , \qquad (4)$$

in which μ_s = coefficient of static friction, for which a value of about 0.1 is reasonable (Hobbs 1974). Values of τ_f up to about 0.1 x 4kPa = 400 Pa would be required to separate two blocks under a normal load of 4kPa.

Yet another possible cause for apparent adhesion between a block of porous columnar ice seated on an ice surface, or some other "wetting" surface, is the development of a suction bond (Tatinclaux in private communication, 1985) at the contact face when brine drains from the ice block.

The strength of the freeze bond between two smooth ice blocks in water and in air is examined in the discussion that follows.

III. EXPERIMENTS

The experiments were conducted in a cold room at the Iowa Institute of Hydraulic Research (IIHR). For all tests, the air temperature in the cold room was held between -1 to +1°C.

A. Apparatus. Ice blocks of repeatable size and smoothness were produced from mains tap water frozen in smooth aluminum casts. Three sizes of casts were used. The casts were filled with tap water and placed in a freezer box which was maintained at an internal air temperature of -10°C. The base areas of the three sizes of ice blocks were 4.52 x $10^{-3}m^2$, 9.03 x $10^{-3}m^2$ and 19.35 x $10^{-3}m^2$; such that the relative sizes of the base areas were 1:2:4 (see figure 3). Although the base of each block was as smooth and planar as the aluminum mold in which it was cast, the upper surface of each block was rounded due to expansion of the water from which it was formed. The top surface was leveled with a heated iron, using the method suggested by Oksanen and Keinonen (1982). The ice blocks are not porous, thereby excluding the possibility of suction-adhesion to the lower ice slab.

For each experiment, the test block of ice was placed on a smooth lower slab of ice 0.71-m long, 0.28-m wide and 0.05-m thick. The lower slab of ice was prepared in a similar manner as that used to produce the test blocks of ice. It was grown in an aluminum container. The surface in contact with the base of the aluminum container was upward and used during the experiments. The surface which was exposed to air, during the growth of the block, and expanded outwards was leveled using a heated iron. This leveled face was in contact with the base of the glass-sided test tank.

Aluminum frames were constructed to fit over the top of each size of test block of ice, as shown in figure 4. The frames were fitted with a hook which was located at the center of the front face of each test block. The experimental set-up is illustrated in figure 5. A light-weight, stainless-steel-strand cable was attached to the hook and passed around a pulley, which guided the cable to a load cell rigidly mounted on the travelling cross-head of a Tinius Olsen universal testing machine. When the cross-head of the testing machine was moved upward, the increasing cable tension was transduced by way of the load cell. The output voltage from the load cell was fed to a signal conditioner which was connected to the IIHR HP1000 computer. Most tests were conducted with the cross-head moving at a speed of 0.84 mm/second. A brief series of tests was conducted with the cross head moving at a speed of 0.44 mm/second.

The load cell was calibrated periodically throughout the experiments, and was used to a precision of ± 0.10N. A typical time history of tension in the cable is shown in figure 5.

B. Program and Procedure. The program of experiments, which is summarized in table 1, involved series of experiments to determine the effects on freeze-bonding of the following parameters:

(i) period of bonding;

(ii) normal pressure;

(iii) contact area;

(iv) fluid in which bonding occurs: air, distilled water, tap water, water from the Iowa River, and 3%, 12.5% and 25% (by weight) NaCl solutions; and,

(v) loading rate.

In general, the experimental procedure that was adopted conformed to the procedure specified in the IAHR Recommendations on Testing Methods of Ice Properties (1980): in accordance with the section on testing for friction coefficient between ice and some material, a test block of ice was seated on and towed over dry and wet surfaces of ice, which were horizontally aligned. The initial peak resistance (see figure 5) was taken to be the shear strength of the freeze-bond between the test block of ice and the ice slab beneath. (Analogously, for an ice block on a surface other than ice, the initial peak resistance could be associated with static friction.)

For each test, a normally loaded block of ice was placed on the ice surface, and, after a prescribed period, was loaded horizontally, by way of a cable tow, until the freeze-bond sheared. Each test was repeated at least 10 times in order to establish one data point.

IV. PRESENTATION AND DISCUSSION OF RESULTS

The results from the experiments are presented and discussed in terms of the influences on freeze-bonding of the following parameters:

(i) contact period (for σ = 460 Pa);

(ii) normal pressure (for a contact period of 10 seconds);

(iii) fluid at contact (air, pure water, river water, saline water, all at 0°C); and,

(iv) contact area.

Preliminary tests were carried out to examine the influence of loading speed on strength of a freeze-bond between the test ice block and the base ice slab. The range of loading speeds was limited to a relatively narrow range; 0.84 mm/sec to 0.44 mm/sec. For this range, loading speed did not influence

the measured strength of the freeze-bond between the ice block and the ice base, as shown in figure 6.

A. Influence of Contact Period. The force required to shear the freeze-bond between the test block and the ice slab increased with increasing contact period when the freeze-bond formed in water. When the freeze-bond formed in air, its strength increased weakly with increasing contact period, and reached an asymptote of 450.4 Pa within 3 minutes of contact. These results are presented in figure 7.

B. Influence of Normal Pressure. For the range of normal pressures used in the present study, the shear strength of the freeze-bond increased linearly with increasing normal pressure, as shown in figure 8. Significantly stronger bonds formed between the ice block and the ice surface when freeze-bonding occurred in either distilled water or tap water than when it occurred in air.

The data indicate that the following relationships can be written for the strength of freeze-bonding:

$$\tau = F_s/A = k\sigma, \quad \text{for} \quad \sigma < 3.5 \text{ kPa} \tag{5}$$

in which k = a coefficient of proportionality, for distilled water, k = 2.01; for tap water, k = 1.95; and for air, k = 0.48; F_s = force to shear the ice block from the ice base; and, A = base area of the test block of ice.

By way of comparison, if freeze-bonding did not occur, (4) suggests that, for ice blocks contacting in air, $k = \mu_s = 0.1$; μ_s may be less than 0.1 for ice contacting in water, if no freeze-bonding occurs.

The data (figure 8) show that, for the same period of bonding, freeze-bonds formed between the ice blocks in water were about 4 times stronger than those formed between ice blocks in air.

Examination of the test blocks, after they were sheared from their freeze-bonded contact at the ice base, revealed a rounding of the side-edges (parallel to the direction of shear) at the contact surfaces with a protrusion of ice beyond the original rectangular edges. Figure 9 shows a 9.01×10^{-3} m^2 contact-area block (medium-size ice block) prior to, and after, an experiment. The top surface of this block was the contact surface. Note that

the rounded edges indicate that freeze-bonding had occurred between the test block and the ice surface, upon which it was seated. During this test, freeze-bonding occurred in tap water.

A similar comparison is depicted in figure 10 for the largest size test block. For each set of photographs (figures 9 and 10), the differences in the edge conditions of the test blocks show that the test block had freeze-bonded to the ice base.

C. Influence of Water Salinity. The strength of the bond formed between the test block and the ice surface decreased with increasing salinity of water in which freeze-bonding occurs. This result is evident in figures 11 and 12, for the following test conditions: water temperature = 0°C, rate of loading = 0.84 mm/sec. In figure 11, normal pressure on the test block was 450 Pa.

When freeze-bonding took place in distilled water and in water from the Iowa River, freeze-bond strength increased linearly with period of freeze-bonding up to 3 minutes (figure 11). When freeze-bonding occurred in a 3% (by weight) saline solution, the strength of the freeze-bond reached an asymptotic value of about 650 Pa. For freeze-bonding occurring in saline water with salinities in excess of 12.5%, the strength of freeze-bonding did not increase with time of contact, but remained at about 200 Pa (for σ = 450 Pa).

The influence of normal pressure, σ, on strength of freeze-bonding diminishes with increasing salinity of water, reaching a lower asymptote which is a function of normal pressure, σ. Figure 12 illustrates this trend.

For 2- to 4-minute periods of contact, the freeze-bond formed in 12.5 and 25% saline solutions, at 0°C, was about half the strength of the freeze-bond formed in air, or for a dry surface, at 0°C.

By comparing figures 12 and 8 it can be seen that freeze-bonds formed in 12.5 and 25% saline solutions, at 0°C, are about 60% less strong than are freeze-bonds formed between dry ice blocks.

For freeze-bonding between ice blocks, (5) can be broadened to include the effect of water salinity; i.e.,

$$F_s/A = \tau = 2.01\ (1 - 0.06\ C)\sigma, \text{ for } C < 12.5\% \quad . \qquad (6)$$

and

$$F_s/A = \tau = 0.28\ \sigma, \text{ for } C > 12.5\% \qquad (7)$$

in which C = concentration of salt as % by weight.

D. Influence of Contact Area. For an ice block in contact with an initially dry surface of ice, figure 13 shows that contact area did not influence the strength of the freeze-bond formed between the ice block and the ice surface. However, as shown in figures 14 and 15, tests for which the contact area was submerged in tap water show that the strength of the freeze bond does depend on contact area.

No discernable effect of block size on freeze-bond strength between ice blocks in air is evident in figure 13. For each of the three block sizes tested, the strengths of the freeze-bond incresed almost linearly with normal pressure σ.

It is difficult to discern, from figure 14, the relationship between block size and contact time on strength of freeze-bonding in tap water. It appears that, at first contact, a stronger bond formed for the two smaller tests block. However, with increasing time of contact, the freeze-bond formed by each of the two smaller ice blocks and the ice base strengthened at a slower rate than did the freeze-bond forming between the largest ice block and the lower ice base.

Normal pressure more profoundly influenced the strength of the freeze-bond between the largest ice block and the ice surface, than it did for the smallest ice block; see figure 15. This result was possibly brought about by the squeezing of the water from between the ice block and the ice surface. Consequently, because a greater surface area of ice was in contact, the freeze-bonds became colder and, therefore, stronger than the freeze-bonds formed between the smallest ice block and the ice surface.

V. CONCLUSIONS

Series of laboratory experiments were conducted with the aim of determining the influence on freeze-bonding between ice blocks of pressure normal to the contact plane, period and area of contact, and salinity of the water in which freeze-bonding occurred. Freeze-bonding between ice blocks in air was also investigated. The experiments were conducted with water and air temperatures of approximately 0°C, and normal pressure between ice blocks up to 4 kPa. This range of normal pressures can be associated with contact pressures between ice blocks in a 10-m-thick layer of floating ice rubble under conditions of hydrostatic loading, and in 2- to 3-m-thick layers of floating ice rubble under conditions of passive Rankine-state loading.

The following principal conclusions were arrived at:

1. The strength of freeze-bonds between ice blocks in contact is influenced by normal pressure, contact time and area, and salinity of the water in which bonding, or fusion, occurs.

2. Stronger freeze-bonds develop between ice blocks in distilled water, tap water and water from the Iowa River than between ice blocks contacting in air. However, stronger freeze-bonds develop between ice blocks in air than develop between ice blocks in a 12.5 or 25% (by weight) saline solution at 0°C. Freeze-bonds formed in distilled, or mains tap water at 0°C are about four times stronger than those formed in air at 0°C.

3. For freeze-bonding between ice blocks contacting for less than one minute in distilled water, strength of freeze-bond

$$F_s/A = \tau = 2.01\sigma,$$

and for freeze-bonding in saline solution, strength of freeze-bond

$$F_s/A = \tau = 2.01(1 - 0.06C)\sigma.$$

For the above equations, F_s = force, in kPa, required to shear a freeze-bond; A = contact area ($9.03 \times 10^{-3} m^2$); τ = nominal shear strength of freeze-bond; σ = normal pressure; C = weight concentration of salt (NaCl) in water.

4. The strength of freeze-bonding increases linearly with contact period for ice blocks contacting in distilled water, tap water, or Iowa River water.

5. The strength of freeze-bonding does not increase with contact period for ice blocks contacting in saline (NaCl) solutions with salinity in excess of 3%, for solution temperature at 0°C.

5. The strength of freeze-bonding does not increase with contact period for ice blocks contacting in air at 0°C.

VI. SIGNIFICANCE OF RESULTS TO THE SHEAR STRENGTH BEHAVIOR OF A LAYER OF FLOATING ICE RUBBLE

The conclusions enumerated in section V, are of some significance to the shear strength and deformation behavior of a layer of floating ice rubble.

Because stronger freeze-bonds form between ice blocks in water, it is likely that the shear strength of rubble in water exhibits a more pronounced cohesive character than does ice rubble being sheared in air. Associated with this result, it is likely that the shear strength behavior of ice rubble in water exhibits a greater shear-rate effect (decreasing strength with increasing rate) than does the shear strength behavior of ice rubble in air.

The cohesive component in the shear strength relationship for floating ice rubble may increase with increasing layer thickness of ice rubble, because normal pressures increase.

Contributing to the scatter of data on the shear strength behavior of rubble ice is the time between tests, because different times may enable stronger freeze-bonds to develop.

REFERENCES

Faraday, M. (1859), "On Regellations and the conservation of Force," Phil. Mag. 17 pp. 162-9.

Hobbs, P.V. (1974), "Ice Physics," Oxford University Press, England.

Hobbs, P.V. and Mason, B.J. (1964), "The Sintering and Adhesion of Ice," Phil. Mag. 9, pp. 181-97.

Jensen, D.C. (1956), "On the Cohesion of Ice," M.S. Thesis, Pennsylvania State University.

Kingery, W.D. (1960), "Regellation, Surface Diffusion and Ice Sintering," Journal of Applied PHysics 31, 833-8.

Kuroiwa, D. (1961), "A Study of Ice Sintering," Tellus 13, pp. 252-9.

Mellor, M. (1980), "Ship Resistance in Thick Brash Ice," Cold Regions Science and Technology, Vol. 3, pp. 305-321.

Merino, M.P. (1974), "Internal Shear Strength of Floating Fragmented Ice Covers,"

Nakaya, U. and Matsumoto, A. (1954), "Simple Experiment Showing the Existence of "liquid Water" Film on the Ice Surface," Journal of Colloidal Science 9, pp. 41-9.

Oksanen, P. (1983), "Friction and Adhesion of Ice," Publication 10, Technical Research Centre of Finland, Laboratory of Structural Engineering, Espoo, Finland.

Oksanen, P. and Keinonen, J. (1982), "The Mechanism of Friction of Ice," Wear 78, 3, pp. 315-326.

Pounder, E.R. (1965), "The Physics of Ice," Pergammon, England.

Thomson, W. (1861), "On Crystalization and Liquifaction Influenced by Stresses Tending to Change of Form in Crystals," Proc. Royal Society A11, pp. 473-81.

Uzuner, M.S. (1974), "Hydraulics and Mechanics of River Ice Jams," Ph.D. Dissertation, Department of Mechanics and Hydraulics, The University of Iowa, Iowa City, Iowa.

Uzuner, M.S. and Kennedy, J.F. (1976), "Theoretical Model of River Ice Jams," Journal of Hydraulics Division ASCE, Vol. 102, HY9, PP. 1365-1383.

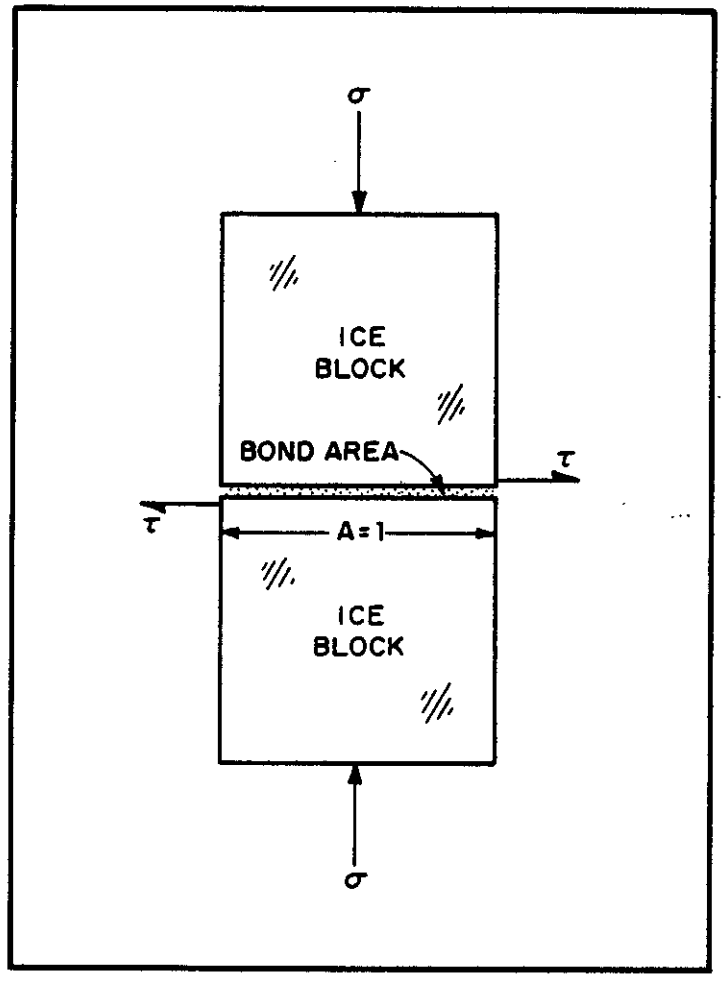

Fig. 1 Contact between two ice blocks

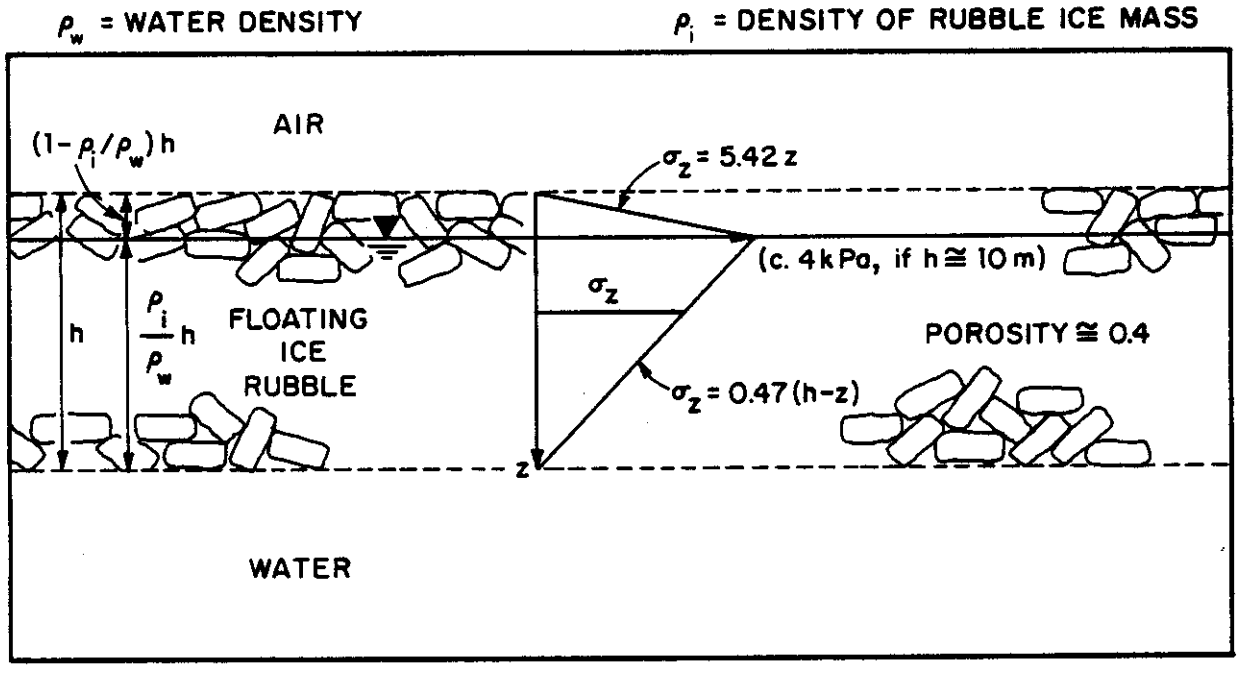

Fig. 2 Pressures within layers of floating ice rubble

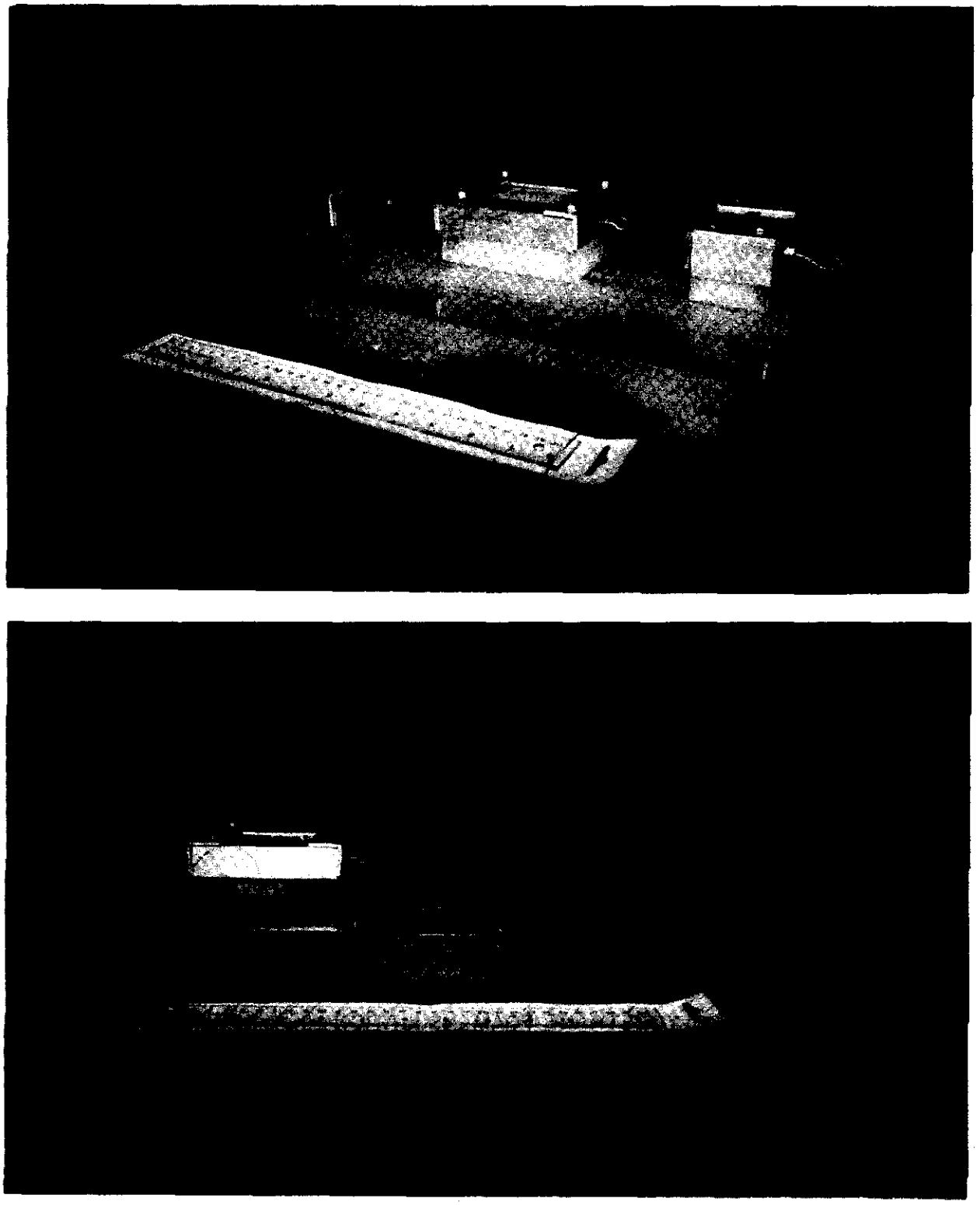

Fig. 3 Samples of the test blocks of ice

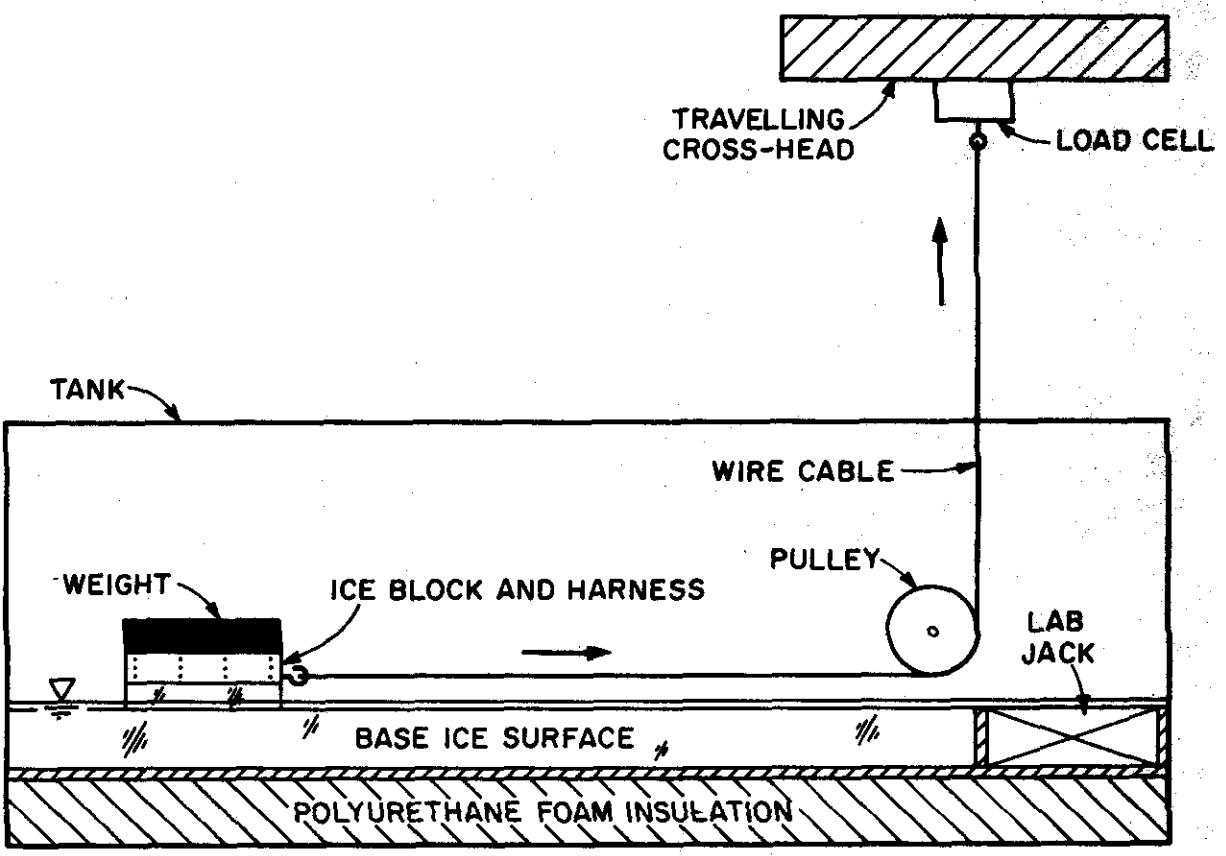

Fig. 4 The experimental set-up

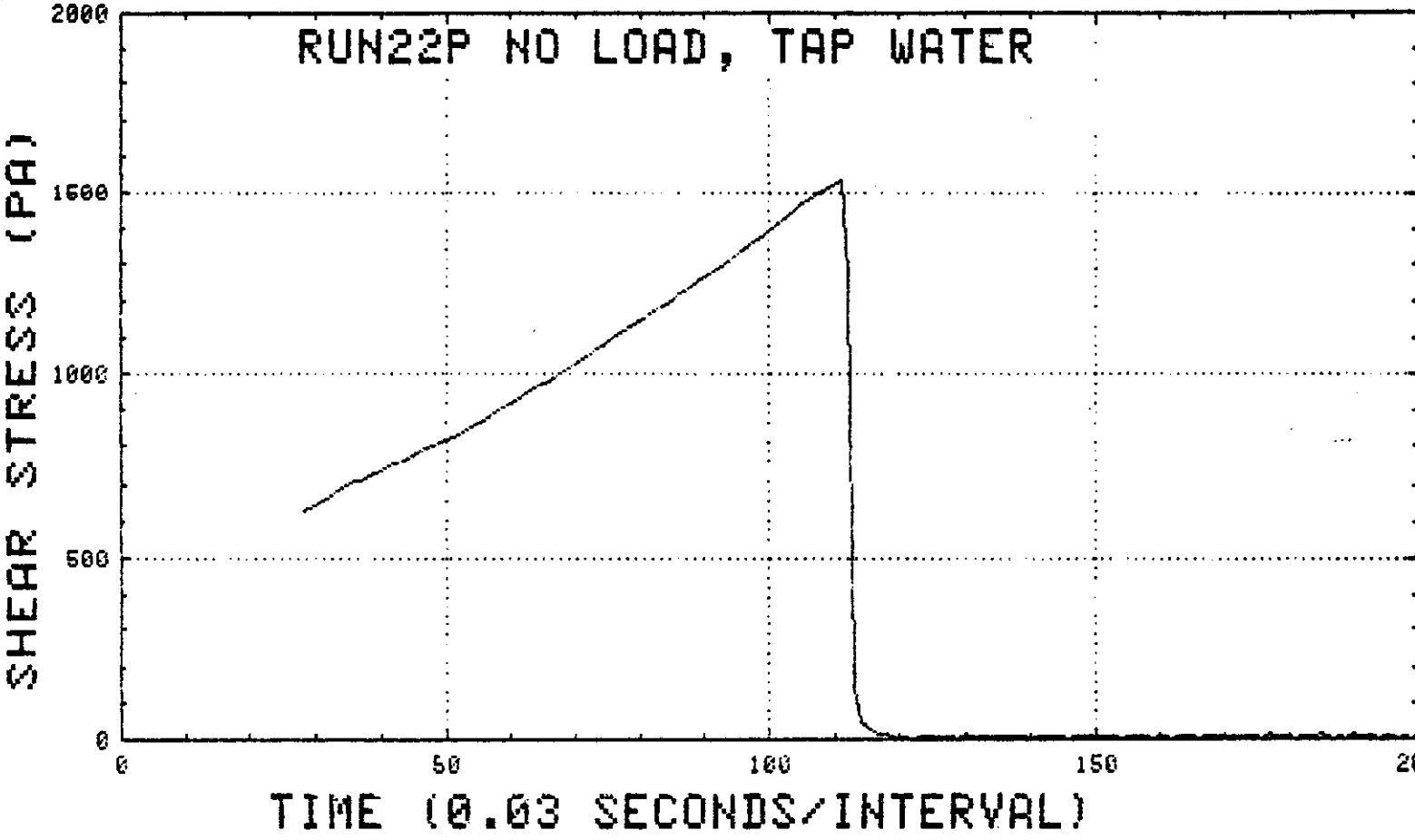

Fig. 5 A typical time history of cable tension

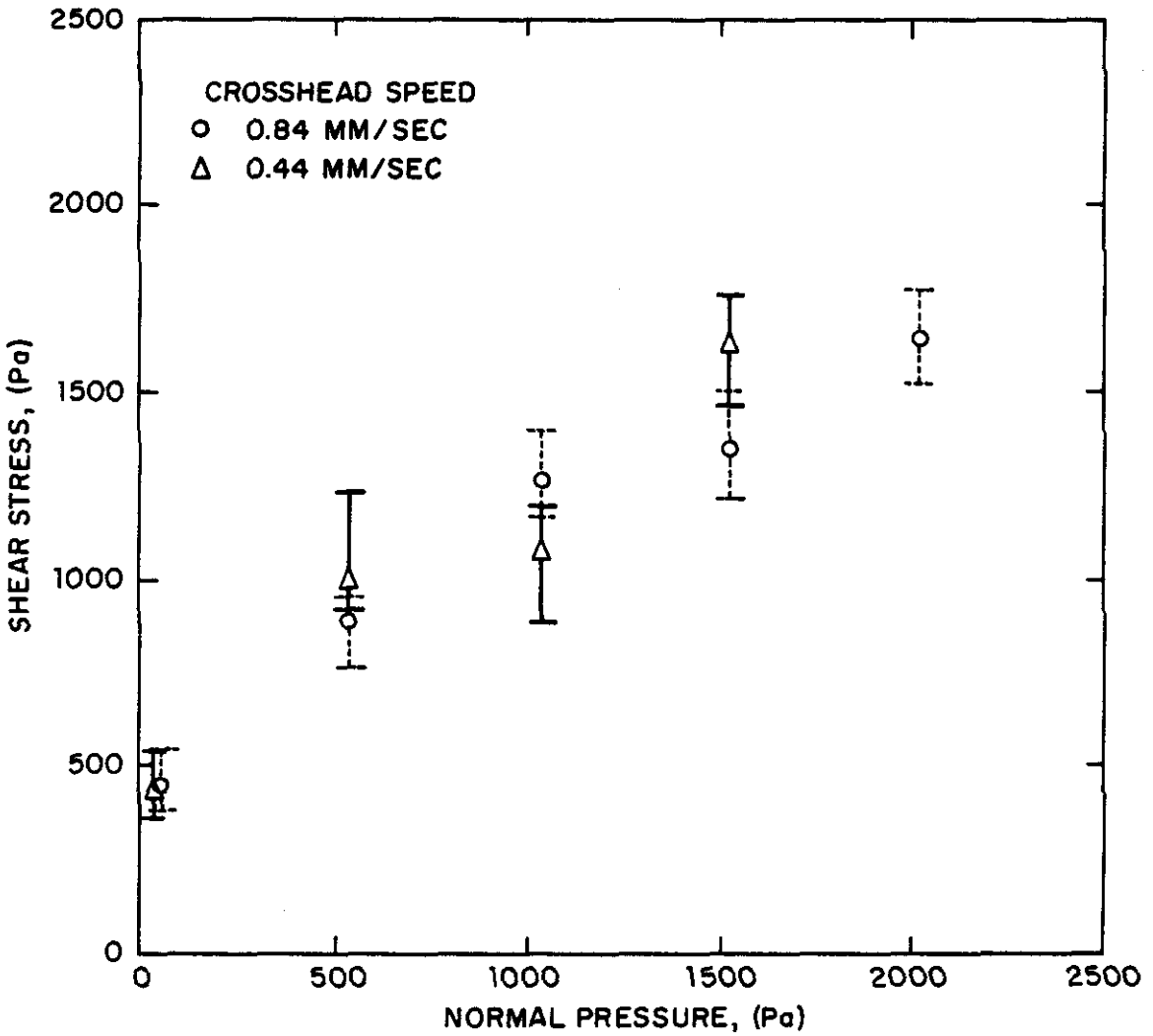

Fig. 6 Influence on freeze-bond strength of the rate of loading rate, for the two speeds tested

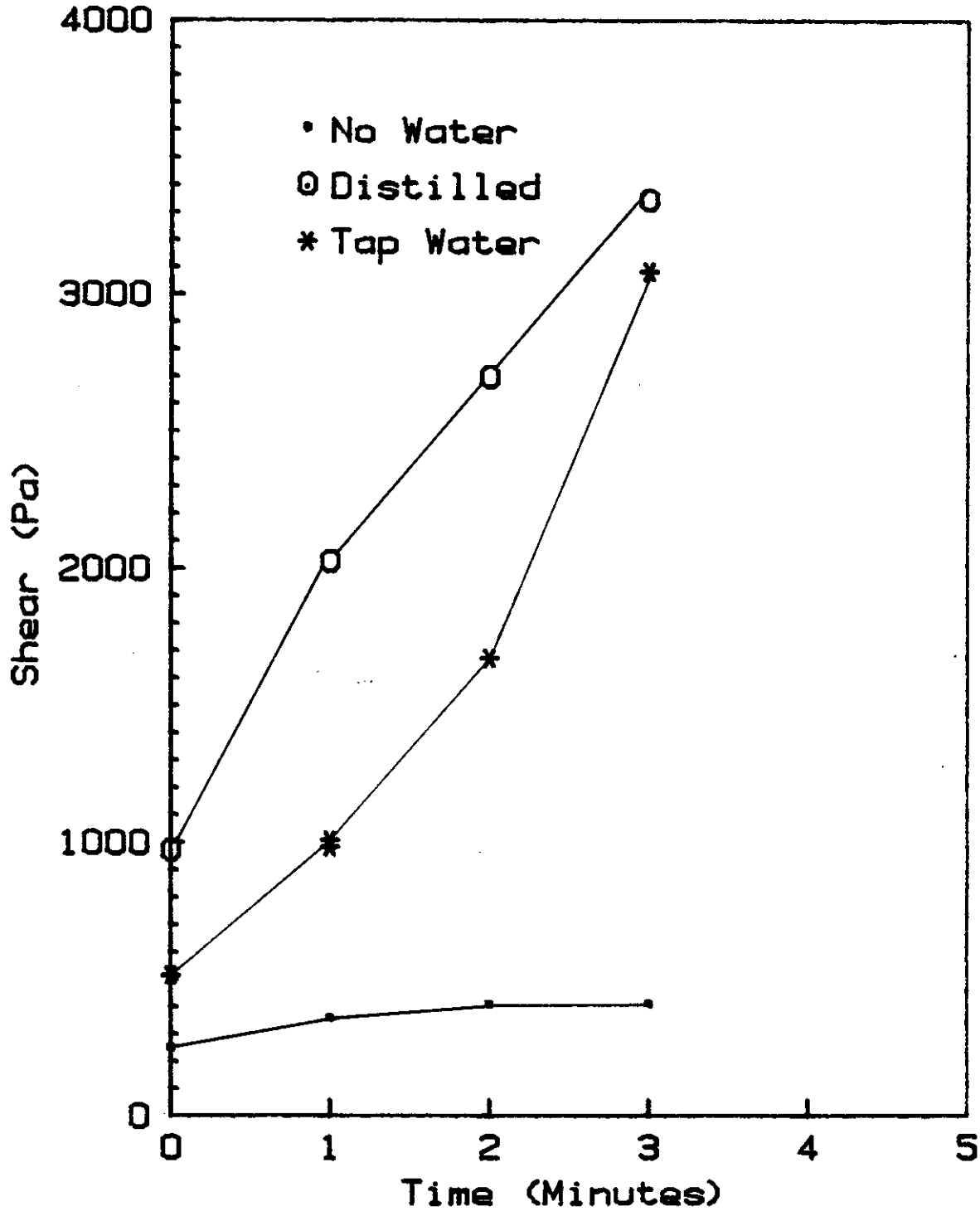

Fig. 7 Strength of freeze-bond versus time of contact

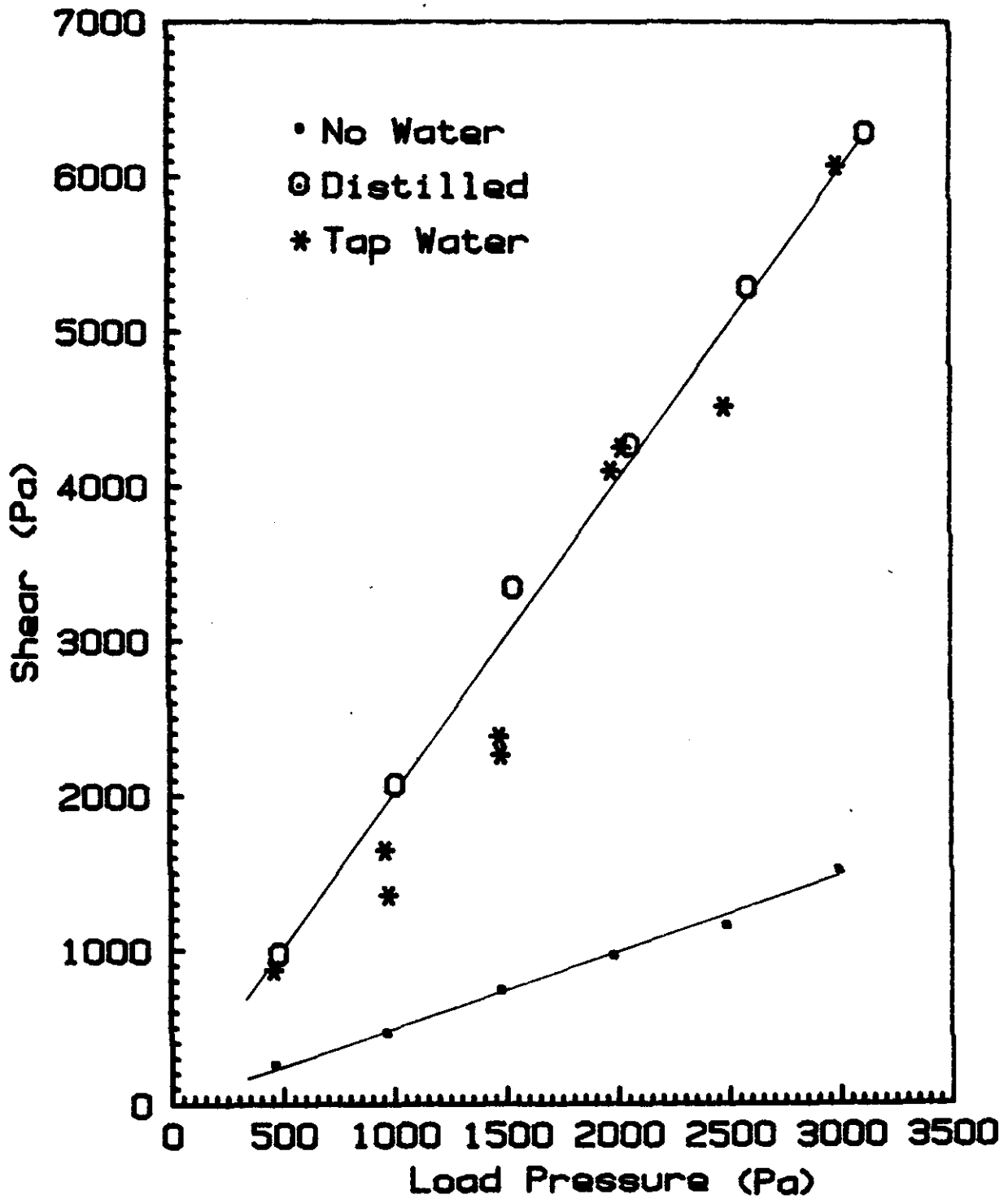

Fig. 8 Strength of freeze-bond versus normal pressure: freeze-bonding in distilled water, tap water and air

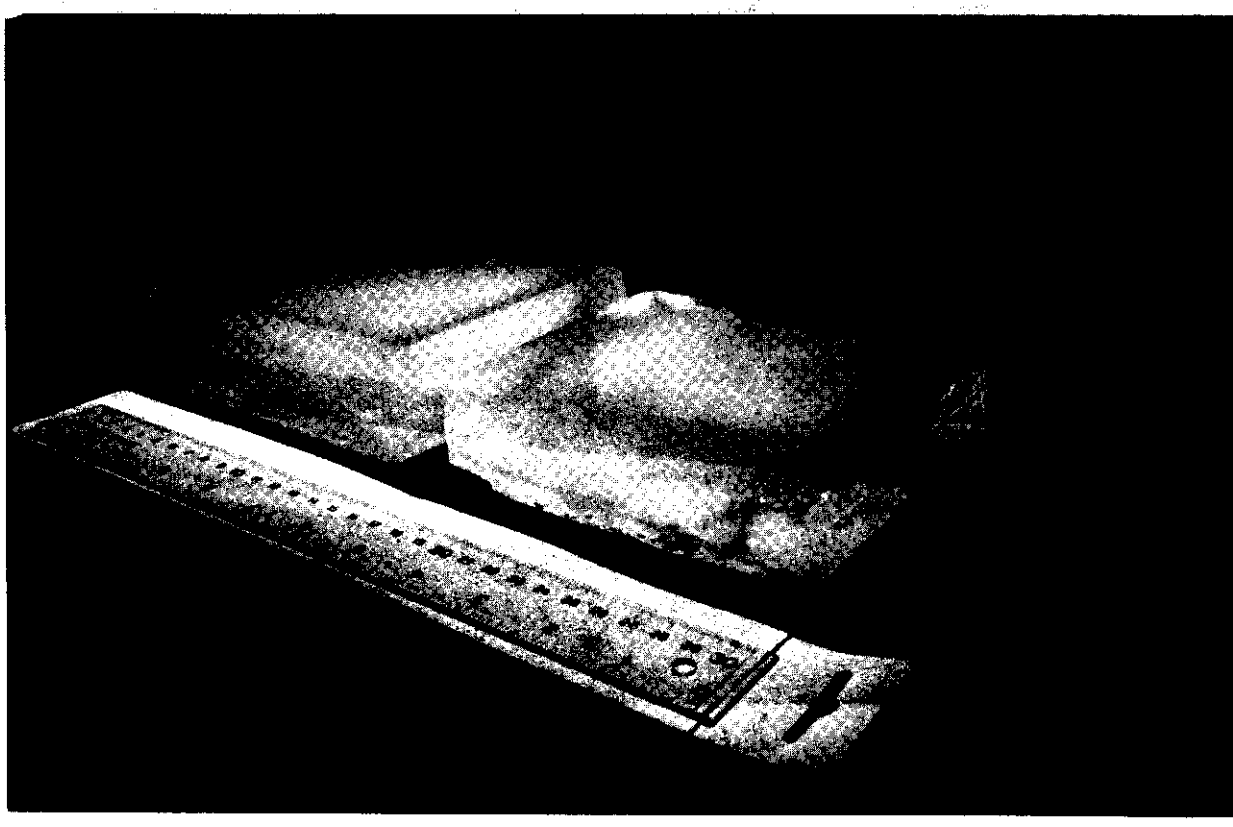

Fig. 10 Condition of a largest-size test block of ice before and after a test

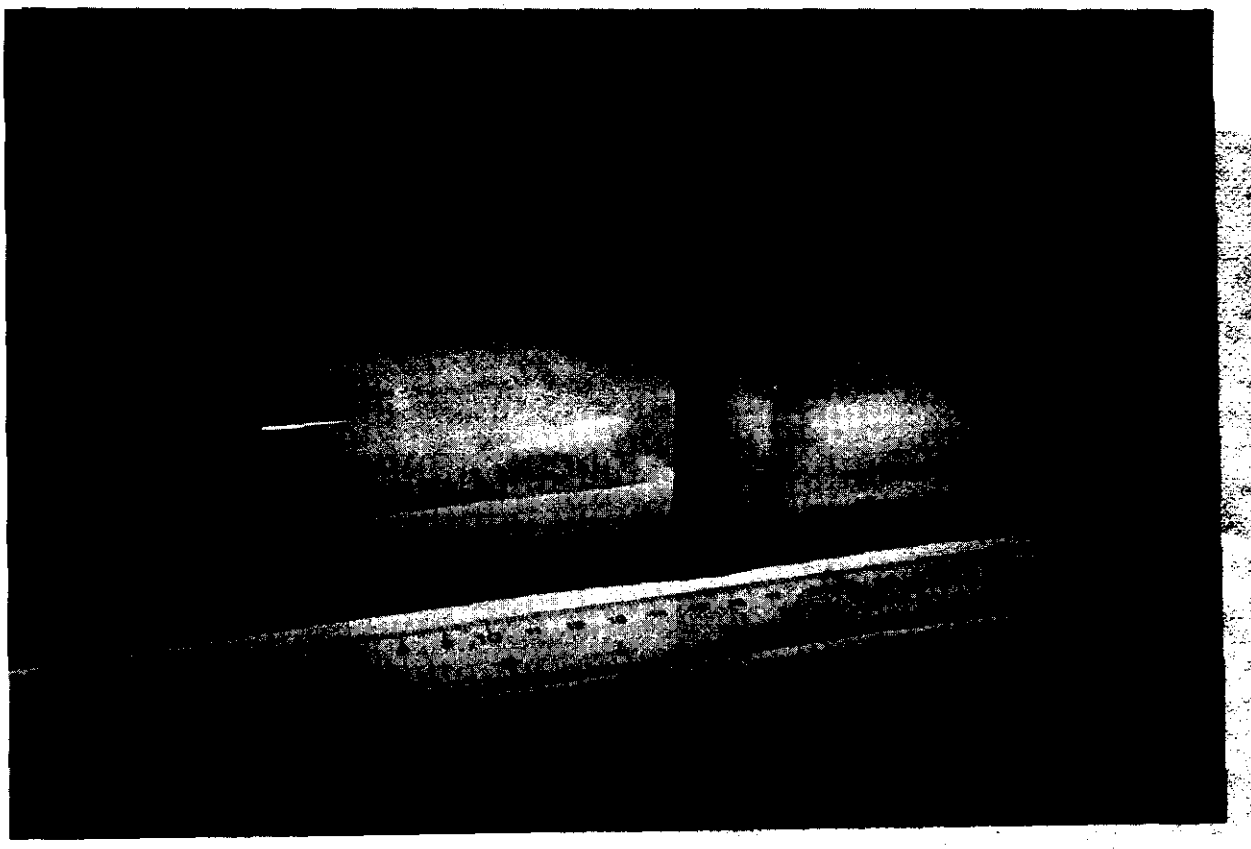

Fig. 9 Condition of a medium-size test block of ice before and after a test

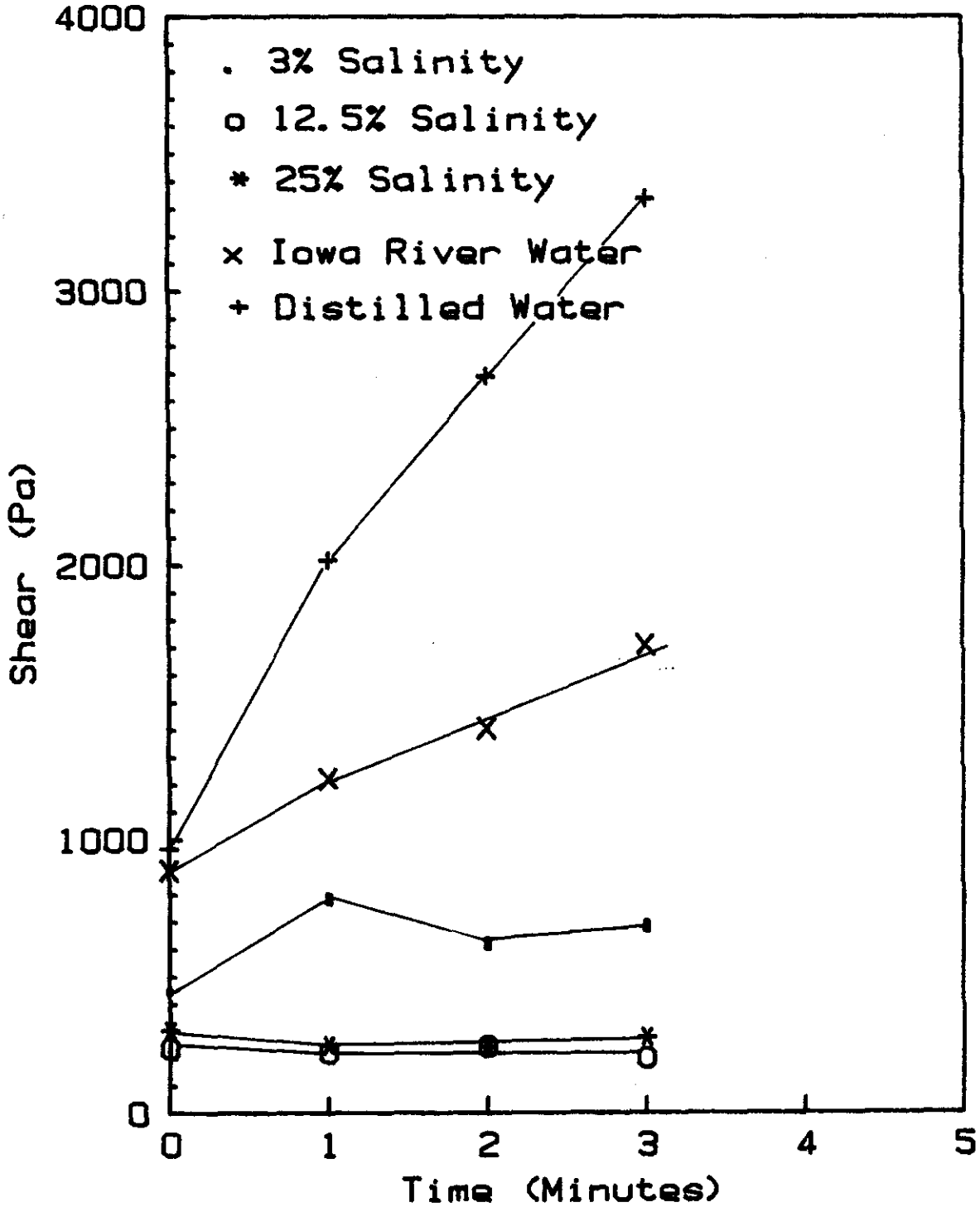

Fig. 11 Strength of freeze-bonding versus contact time for freeze-bonding in saline solutions at 0°C

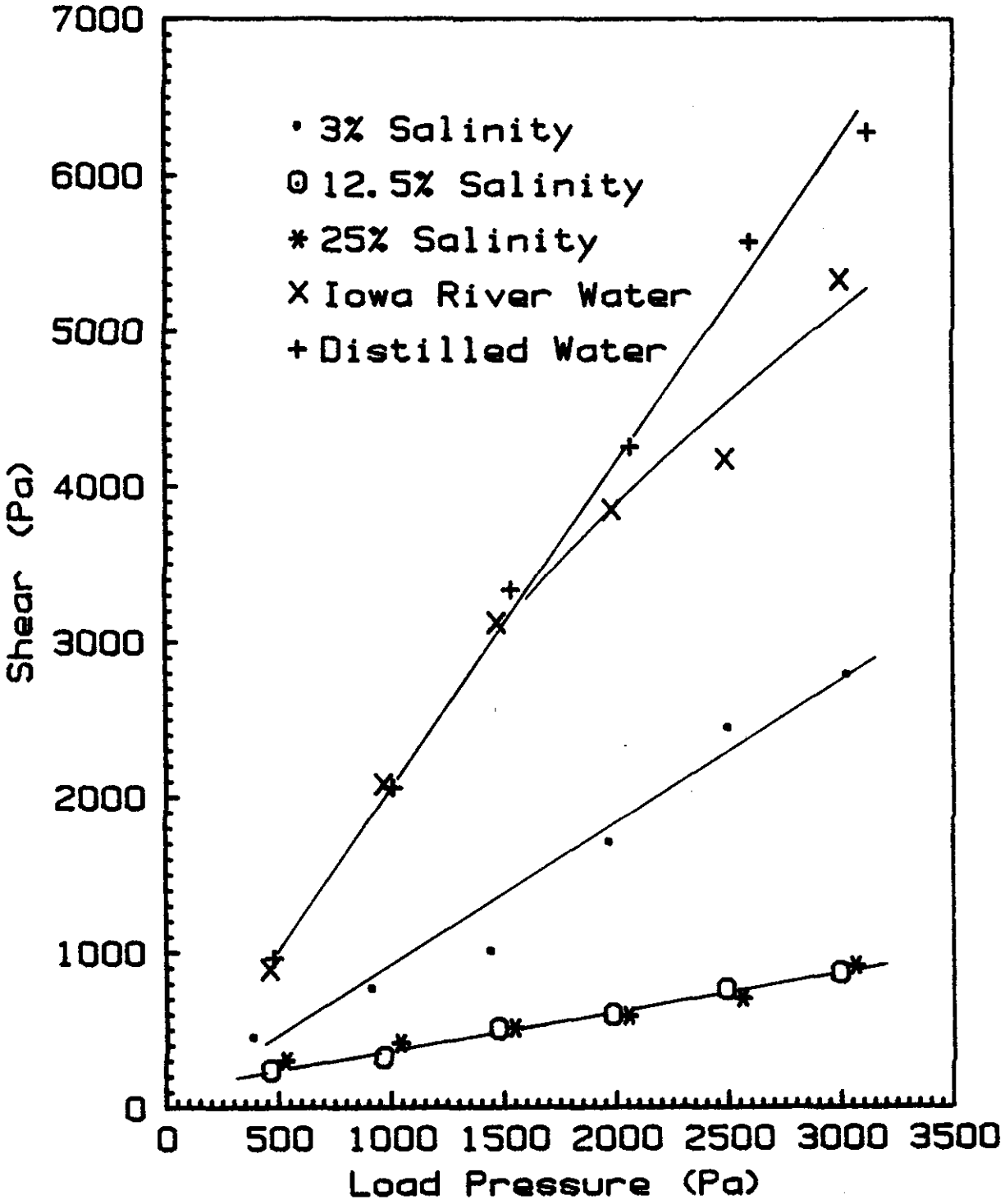

Fig. 12 Strength of freeze-bonding versus noral pressure for freeze-bonding in saline solutions at 0°C

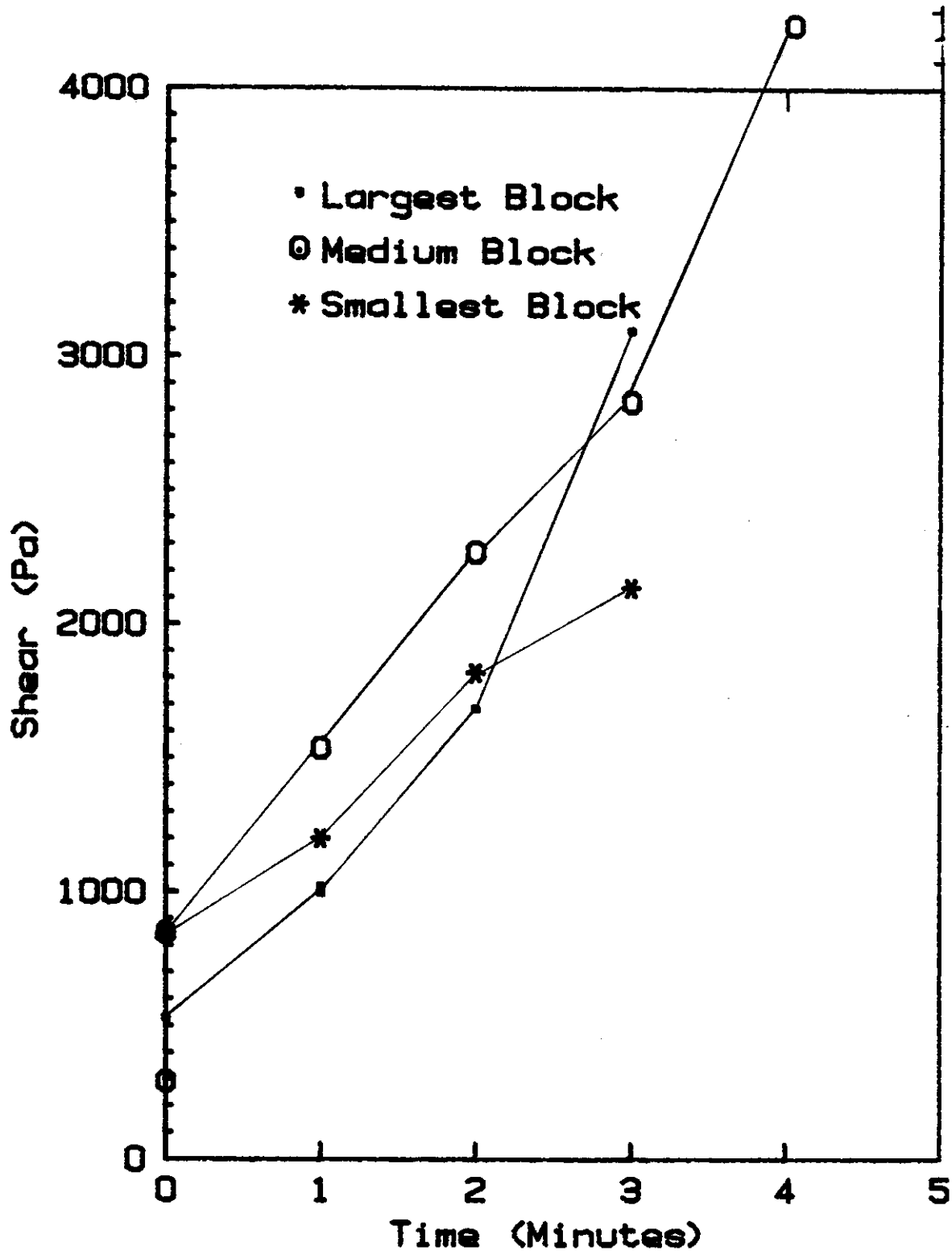

Fig. 13 Strength of freeze-bonding versus contact time for three sizes of test ice block: freeze-bonding in tap water at 0°C

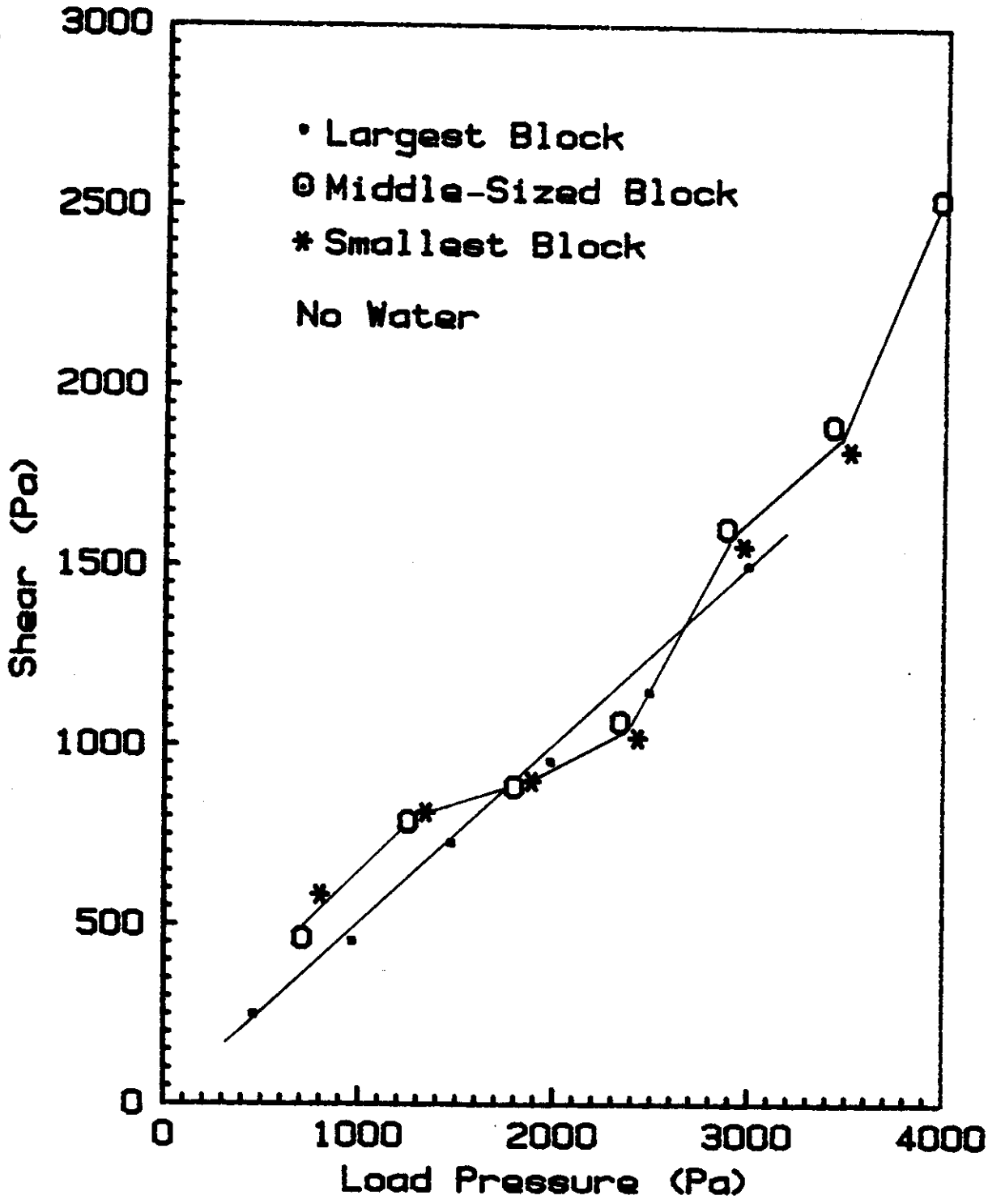

Fig. 14 Strength of freeze-bonding versus normal pressure for three sizes of test ice block: freeze-bonding in air at 0°C

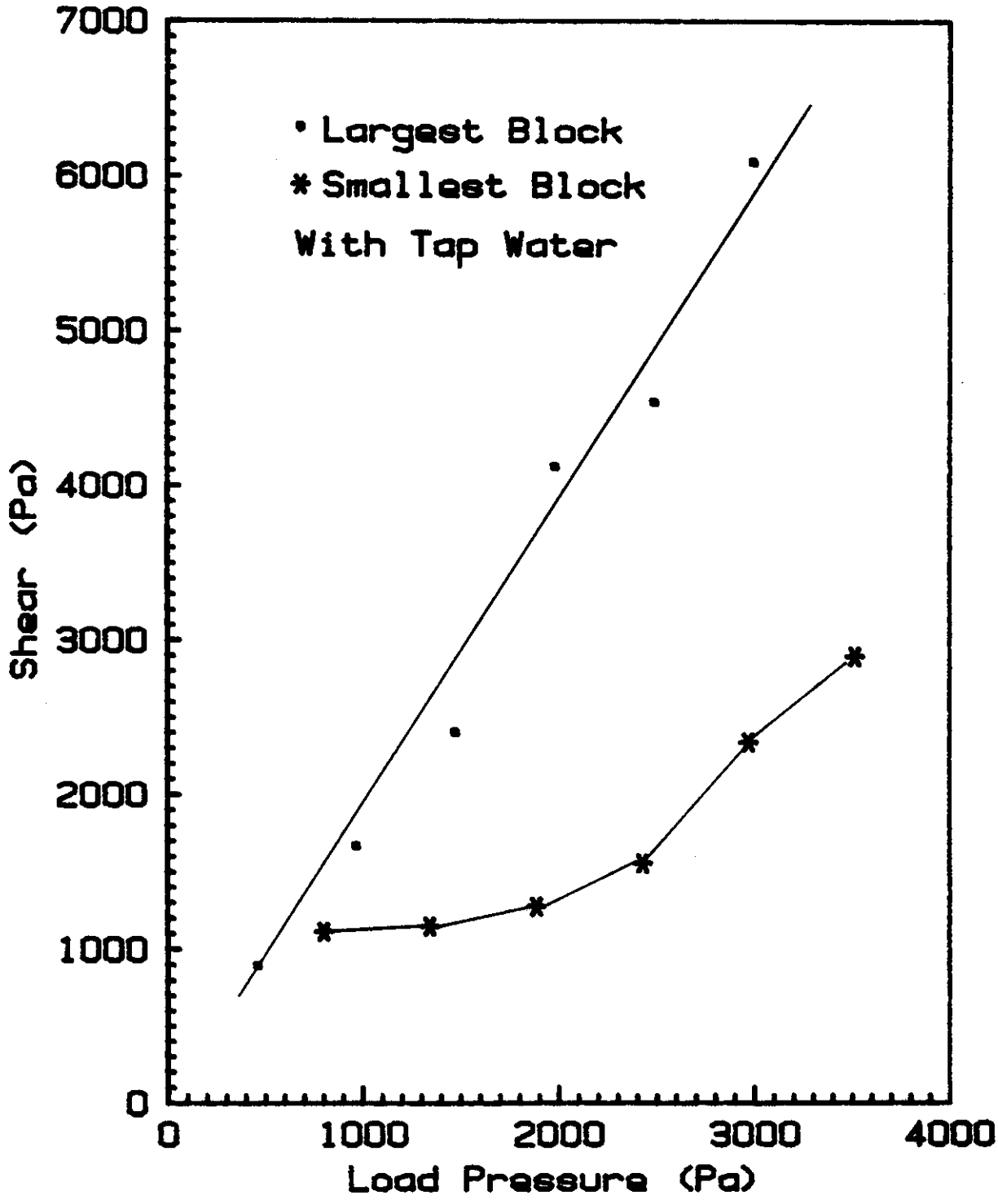

Fig. 15 Strength of freeze-bonding versus normal pressure for two sizes of test ice block: freeze-bonding in tap water at 0°C

Table 1: Program of Experiments

1. Effect of Loading Rate

    a. Cross-head Speed of 0.84 min/second
    b. Cross-head Speed of 0.44 min/second

2. Effect of Period of Bonding (0 to 4 minutes)

    a. In air
    b. In Distilled Water
    c. In Tap Water
    d. In 3% Salinity Water
    e. In 12.5% Salinity Water
    f. In 25% Salinity Water
    g. In Iowa River Water

3. Effect of Normal Pressure (0 to 4kPa)

    a. In air
    b. In Distilled Water
    c. In Tap Water
    d. In 3% Salinity Water
    e. In 12.5% Salinity Water
    f. In 25% Salinity Water
    g. In Iowa River Water

4. Effect of Contact Area using Blocks having area ratios of 1:2:4

    a. In Air
    b. In Tap Water

APPENDIX 1: Summary of Data

(each value tabulated is the average of ten tests)

Reference Figure	Run No.	Normal Pressure σ (Pa)	Contact Time (minutes)	Strength of Freeze-bond τ (Pa) Mean	Max.	Min.	2 Std. Deviation
7	AIR						
	240	460.33	0.17	240.16	302.78	125.49	39.42
	246	460.33	1	347.70	583.63	234.14	61.91
	247	460.33	2	398.40	510.20	341.14	51.68
	248	460.33	3	400.72	494.99	356.21	29.55
	121	460.33	1	337.60	573.84	207.20	77.95
	122	460.33	2	370.98	624.11	159.09	83.45
	123	460.33	3	323.64	403.83	287.37	24.41
	124	460.33	4	420.42	524.51	320.28	66.96
7	DISTILLED WATER						
	311	460.33	0.17	965.91	1533.44	446.6	172.25
	317	460.33	1	2021.10	2798.2	1322.34	268.3
	318	460.33	2	2692.26	3626.80	1835.27	375.52
	319	460.33	3	3340.14	3975.79	2806.92	262.44
7	TAP WATER						
	130	380.87	0.17	515.90	828.73	261.71	103.19
	131	380.87	1	985.07	1210.83	732.78	152.85
	132	380.87	2	1673.39	2479.20	980.48	368.81
	133	380.87	3	3084.32	4412.43	1402.75	743.80
	134	380.87	1	1009.06	1678.39	504.22	409.74
8	AIR						
	240	460.33	0.17	240.16	302.78	125.49	39.39
	241	967.31	0.17	444.55	494.99	311.13	32.39
	243	1981.27	0.17	947.08	1036.84	804.48	44.28
	244	2488.24	0.17	1142.07	1257.55	1051.90	45.41
	245	2995.22	0.17	1492.24	1755.96	1207.40	131.52
8	DISTILLED WATER						
	311	480.19	0.17	965.91	1533.43	568.71	172.25
	313	1537.87	0.17	3334.82	4722.35	2383.04	536.38
	314	2066.71	0.17	4253.05	5729.02	2133.52	625.60
	315	2595.55	0.17	5572.83	8958.09	4359.5	863.89
	316	3124.39	0.17	6275.20	7946.28	4944.01	658.53

8	TAP WATER						
	251	460.33	0.17	873.23	1378.65	575.27	195.38
	255	967.31	0.17	1648.17	3431.64	1015.19	427.18
	256	1474.29	0.17	2380.57	3741.13	1638.96	404.08
	257	1981.27	0.17	4098.55	5875.08	2659.08	675.19
	258	2488.24	0.17	4511.95	7187.84	3130.78	794.47
	259	2995.22	0.17	6070.59	8425.52	4301.33	965.48
	161	467.94	0.17	683.93	917.54	311.95	66.52
	162	974.92	0.17	1358.02	1914.30	870.56	315.07
	163	1481.89	0.17	265.64	2802.17	1369.75	291.41
	164	1988.87	0.17	2940.19	3921.07	2164.34	354.88
	165	2495.87	0.17	4251.03	4891.60	2983.73	390.57
11	WATER-3% SALINITY						
	135	380.81	0	432.03	575.75	228.55	60.92
	13B	380.81	1	758.95	1261.43	505.96	174.36
	13C	380.81	2	597.15	793.84	378.60	81.64
	13D	380.81	3	682.88	1057.30	380.34	157.59
11	WATER-12% SALINITY						
	249	380.81	0	150.46	220.85	88.63	147.80
	24F	380.81	1	214.05	356.21	128.78	53.12
	24G	380.81	2	237.82	322.78	178.93	27.21
	24H	380.81	3	194.68	235.78	130.43	34.93
11	WATER-25% SALINITY						
	233	380.81	0	302.48	561.85	185.64	65.22
	239	380.81	1	251.11	342.78	205.78	28.94
	23A	380.81	2	244.29	378.35	190.71	33.80
	23B	380.81	3	278.81	387.99	197.42	41.29
11	IOWA RIVER WATER						
	26D	380.81	0	880.88	1390.73	667.28	175.91
	26E	380.81	1	1214.99	1493.47	777.67	232.15
	26F	380.81	2	1400.03	2336.31	898.08	306.06
	26G	380.81	3	1702.26	2087.10	1133.89	228.16
12	WATER-3% SALINITY						
	31C	380.81	1	782.19	1056.95	633.84	77.88
	31D	380.81	2	620.16	801.08	508.40	60.93
	31E	380.81	3	660.52	923.16	418.10	81.50

	WATER-3% SALINITY						
	135	380.81	0.17	432.03	575.75	228.55	60.92
	136	909.70	0.17	747.09	1107.89	481.53	137.32
	137	1438.60	0.17	988.19	1268.41	345.45	172.03
	138	1967.50	0.17	1690.64	2322.27	1278.88	236.04
	139	2496.40	0.17	2427.43	3063.77	1793.58	248.98
	13A	3025.30	0.17	2768.01	3527.85	1664.52	395.51
12	WATER-12.5% SALINITY						
	249	466.33	0.17	150.46	220.85	88.65	26.51
	24A	967.31	0.17	314.42	416.49	199.06	47.84
	24B	1474.29	0.17	449.10	515.13	369.63	33.01
	24C	1981.27	0.17	588.99	685.70	449.37	43.62
	24D	2488.24	0.17	752.14	923.26	657.34	59.20
	24E	2995.22	0.17	856.95	1053.55	595.28	87.60
12	WATER-25% SALINITY						
	233	532.33	0.17	302.48	561.85	185.64	65.22
	234	1039.30	0.17	417.45	521.70	356.20	38.30
	235	1546.28	0.17	514.99	588.70	419.78	34.75
	236	2053.26	0.17	590.48	832.98	448.13	68.79
	237	2560.24	0.17	705.43	948.19	503.35	66.41
	238	3064.21	0.17	913.95	1152.33	628.84	118.24
12	WATER-IOWA RIVER WATER						
	260	460.33	0.17	880.88	1577.04	667.28	175.91
	26H	967.31	0.17	2273.56	2993.64	1351.30	678.24
	26I	1474.29	0.17	3111.33	4605.75	2488.51	502.77
	26J	1981.27	0.17	3836.07	5602.58	2951.72	600.27
	26K	2488.24	0.17	4160.77	5532.30	2981.86	576.07
	31F	2995.22	0.17	5320.41	7383.62	4256.26	855.30
13	LARGE BLOCK IN TAP WATER						
	130	380.87	0	515.90	828.73	261.71	103.19
	131	380.87	1	985.07	1210.83	732.78	152.85
	132	380.87	2	1673.39	2479.20	980.48	368.81
	133	380.87	3	3084.32	4412.43	1402.75	743.80
	134	380.87	1	1009.06	1678.39	504.22	409.74
13	MEDIUM BLOCK IN TAP WATER						
	292	380.87	0	842.86	1236.37	670.15	102.87
	293	380.87	1	1531.01	2436.92	949.69	355.22
	294	380.87	2	2265.23	3544.35	1229.21	578.05
	295	380.87	3	2825.36	4174.96	2110.79	370.08
	296	380.87	4	4252.16	5913.23	2924.29	1253.58

14	SMALLEST BLOCK IN TAP WATER						
	307	380	0	869.99	1152.66	529.80	141.09
	308	380	1	1357.14	1847.14	665.86	404.33
	309	380	2	1359.57	1782.74	630.02	495.29
	30A	380	3	1970.05	2140.68	766.09	499.38
14	LARGEST BLOCK IN AIR						
	240	460.33	0.17	240.16	302.78	125.49	39.39
	241	967.31	0.17	444.55	494.99	311.13	32.39
	242	1474.29	0.17	721.03	857.91	563.63	52.17
	243	1981.27	0.17	947.08	1036.84	804.48	44.28
	244	2488.24	0.17	1142.07	1257.55	1051.90	45.41
	245	2995.22	0.17	1492.24	1755.96	1207.40	131.52
14	MIDDLE SIZED BLOCK IN AIR						
	260	708.86	0.17	456.48	845.77	240.11	110.11
	261	1252.05	0.17	782.95	1064.36	612.81	75.39
	262	1795.24	0.17	881.06	1110.95	784.82	71.30
	263	2338.43	0.17	1063.68	1243.53	820.67	91.17
	264	2881.62	0.17	1602.66	1996.12	1304.48	132.21
	265	3424.81	0.17	1889.48	2186.06	1576.83	105.66
	266	3968.00	0.17	2520.04	3368.80	1885.03	260.33
14	SMALLEST BLOCK IN AIR						
	300	800.86	0.17	582.58	859.11	372.29	104.29
	301	1343.45	0.17	813.97	1081.10	551.28	126.64
	302	1886.04	0.17	901.66	1073.95	730.26	77.97
	303	2428.63	0.17	1023.67	1202.80	849.95	60.89
	304	2971.21	0.17	1599.97	2226.61	1338.81	177.10
	305	3513.80	0.17	1824.35	2269.53	1174.18	203.46
15	LARGEST BLOCK IN TAP WATER						
	251	460.33	0.17	873.23	1378.65	575.27	195.38
	255	967.31	0.17	1648.17	3431.64	1015.19	427.18
	256	1474.29	0.17	2380.57	3741.13	1638.96	404.08
	257	1981.27	0.17	4098.55	5875.08	2659.08	675.19
	258	2488.24	0.17	4511.95	7187.84	3130.78	794.47
	259	2995.22	0.17	6070.59	8425.52	4301.33	965.48
	161	467.94	0.17	683.93	917.54	311.95	66.52
	162	974.92	0.17	1358.02	1914.30	870.56	315.07
	163	1481.89	0.17	2265.64	2802.17	1369.75	291.41
	164	1988.87	0.17	2940.19	3921.07	2164.34	354.88
	165	2495.87	0.17	4251.03	4871.60	2983.73	390.57

15 SMALLEST BLOCK IN TAP WATER

30B	543.05	0.17	1115.34	1911.59	673.01	230.94
30I	1086.10	0.17	1150.32	1482.04	751.72	119.55
30D	1629.16	0.17	1276.76	1639.51	923.57	143.69
30J	2172.22	0.17	1559.08	1754.06	1195.65	128.46
30K	2715.27	0.17	2341.61	3973.51	1839.98	455.94
30G	3258.33	0.17	2986.29	4831.04	2004.67	371.41